

## MiR-122-3p Targets Enhancer of Zeste Homologue 2 to Mitigate Steroid-induced Osteonecrosis in the Femoral Head

Changde Wang, Chunzhu Gong, Yiming Luo, Mina Kai, Yong Sun and Yun Lu

*Department of Geriatric Orthopedics, Shenzhen Pingle Orthopaedic Hospital, Shenzhen 518000, China*

**KEYWORDS** Enhancer of Zeste Homologue 2. Femoral Head. Mir-122-3p. Osteonecrosis. Steroid

**ABSTRACT** The researchers aimed to unravel the mechanism by which miR-122-3p targeting enhancer of the zeste homologue 2 (EZH2) alleviates steroid-induced osteonecrosis in the femoral head (ONFH). BMS cell suspension was transfected using miR-122-3p mimics and miR-NC vectors, and injected into mice. The mice were divided into normal, ONFH, miR-122-3p and miR-NC groups. MiR-122-3p targeted EZH2 and regulated its expression negatively. The overexpression of miR-122-3p was capable of improving trabecular parameters and increasing the expressions of miR-122-3p and EZH2. EZH2 reversed the influence of miR-122-3p overexpression on steroid-induced ONFH. MiR-122-3p plays an inhibitory role in ONFH, with its expression down-regulated. The overexpression of miR-122-3p can improve ONFH tissues and adjust trabecular parameters, probably by targeting and negatively regulating EZH2 expression.

### INTRODUCTION

Osteonecrosis of the femoral head (ONFH) is a blood circulation disorder (Chikvatia et al. 2020). Many factors contribute to the differentiation of osteocytes and bone marrow, which leads to ischemic necrosis (Hua et al. 2019). Under continuous stress, the femoral head collapses to make the hip joint no longer function (Chen et al. 2020; Wang et al. 2020). According to the aetiology, ONFH can be classified into traumatic ONFH (generally caused by trauma of the hip joint) and non-traumatic ONFH (usually induced by heavy use of hormones or alcoholism for a long time) (Baba et al. 2020). Glucocorticoid is the primary contributor to non-traumatic ONFH (Naik et al. 2020). When ONFH patients use glucocorticoids at high doses for a long time, the local microcirculation in their femoral head is damaged, thereby inducing the endoplasmic reticulum stress and massive apoptosis of osteoblasts, and disturbing the balance between the osteogenic differentiation of bone marrow mesenchymal stem cells (BMSCs) and their adipogenic differentiation (Kang et al. 2018). Over 70 percent of the cases suffering from steroid-induced ONFH (SIONFH) need hip replacement surgery (Pavelka et al. 2019; Lai et al. 2020). However, the postoperative quality of life is seriously affected, and there is a high risk of infection. Hence, finding new drugs to prevent and to treat

SIONFH has attracted widespread attention.

Micro ribonucleic acids (miRNAs) are single-stranded non-coding RNA molecules. They can specifically bind target gene 3'-untranslated region (3'-UTR) to repress messenger RNA (mRNA) translation or directly influence the degradation, thus modulating the expressions of target genes (Liao et al. 2019). MiR-122-3p is a miRNA mediating many diseases (Hao et al. 2019). Wang et al. (2018) found that the miR-122-3p expression in SIONFH plummeted during the osteogenic differentiation of BMSCs. MiRNAs play biological roles by targeting their downstream genes.

It has been reported that there may be a targeting relationship between enhancer of zeste homologue 2 (EZH2) and miR-122-3p (Aranza-Martínez et al. 2021). As a catalytic subunit of polycomb group protein inhibitory complexes, EZH2 can promote diseases by suppressing the expressions of genes related to cell proliferation, differentiation and cycle regulation (Chu et al. 2020). Inhibiting the expression and activity of EZH2 can reduce the H3K27me3 content, thus facilitating human embryonic stem cell differentiation into BMSCs (Deng et al. 2020). The expression and function of EZH2 have been implicated in bone metabolic diseases (Xu et al. 2021). However, their relationship with SIONFH has seldom been reported.

### Objectives

The objective of this study was to explore the expressions of miR-122-3p and EZH2 in

\*Address for correspondence:  
Changde Wang  
E-mail: wangcdspoh@sdsch.cn

SIONFH, and to provide experimental reference for clinical treatment.

## MATERIAL AND METHODS

### Laboratory Animals

Fifty BALB/c male mice (SPF, 8-week-old, 16-26 g) were purchased from Beijing Vital River Laboratory Animal Technology Co., Ltd., with an animal production licence: SCXK (Beijing) 2016-0006. The mice were raised with at 22-26°C and a relative humidity range of 40 percent to 60 percent. They were provided with unlimited food and water, and their diet was adjusted according to their needs for a period of one week. The research adhered to the ethical principles and welfare guidelines for laboratory animals, and received approval from the hospital's ethics committee.

### Main Reagents and Apparatus

MiR-122-3p mimics lentiviral vector, miR-NC empty vector (Shanghai Genechem Co., Ltd.), EZH2 antibody (Shanghai Kang Lang Biotechnology Co., Ltd.), bicinchoninic acid protein assay kit and trypsin (Shanghai Zhennuo Biotechnology Co., Ltd.), along with micro-computed tomography (micro-CT) system (GE Healthcare Life sciences) were used.

### Animal Grouping and Model Establishment

A total of 40 mice were randomly divided into four groups: the Normal group (consisting of normal mice injected with 1 mL of normal saline, n=10), the ONFH group (treated with intramuscular injection of 1 mL of normal saline, n=10), the miR-NC group (transfected with BMSCs suspension containing miR-NC empty vector following the treatment in the ONFH group, n=10), and the miR-122-3p group (transfected with BMSCs suspension containing miR-122-3p mimics lentivirus following the treatment in the ONFH group, n=10). The SIONFH mice model was created by administering lipopolysaccharide intravenously at a dosage of 10 µg/kg for two consecutive days, except for the Normal group. This was followed by three intramuscular injections of methylprednisolone with a 24-hour interval. Increased empty bone lacunae, reduced trabeculae,

and trabecular damage indicated successful modelling. During the 6<sup>th</sup> week after drug intervention, follow-up experiments were conducted.

### Isolation, Culture and Identification of BMSCs

The remaining 10 mice provided BMSCs. In particular, the femoral bone marrow was obtained from the mice, aseptically placed into a centrifuge tube with an equal amount of phosphate-buffered saline, and subsequently agitated to create a cell suspension. Afterward, the suspension was placed into a tube designed for centrifugation. Following centrifugation at a speed of 2,000 revolutions per minute for a duration of 20 minutes, the mononuclear cells present in the white membrane layer were transferred to a separate tube. Subsequently, they were rinsed twice with low-glucose Dulbecco's modified Eagle medium (DMEM) and the liquid above was removed. Afterward, the cells were suspended again using DMEM complete medium, and the density of the cells was modified to  $1 \times 10^6$ /mL. Ultimately, the cells were introduced into a culture flask to undergo incubation, and the resulting cells were identified as primary BMSCs. The medium for culturing cells was changed every other day. After reaching a fusion rate of 90 percent, the cells were digested and passed. For immunofluorescence staining, the CD29, CD34, and CD90 clusters of differentiation were chosen in the third-gen cells.

### Transfection of Lentivirus Into BMSCs

Prior to transfection, the cells were diluted to a density of  $3$  to  $5 \times 10^3$ /mL, and subsequently introduced into a 96-well plate. Afterward, 100 µL of culture medium was introduced into every well of the well plate. According to the ideal infection complex value, lentivirus, miR-122-3p imitations, and miR-NC were separately transfected into various groups using 5 µg/mL polybrene to aid in cell transfection. Afterward, the cells were co-cultured for a duration of 24 hours.

### Injection of BMSCs

After four weeks of developing steroid-induced ONFH, the mice in every group were given anesthesia through intraperitoneal injection of chloral hydrate. Specifically, a cut was made

in the knee's skin along the central longitudinal line of the knee joint to locate the patellar ligament. Next, 200  $\mu$ L of BMSCs (approximately  $10^6$ ) were administered into the femoral medullary cavity in both the miR-NC group (transfected with miR-NC) and the miR-122-3p group (transfected with miR-122-3p mimics). Oral amoxicillin was given with drinking water to resist infection.

#### **Detection of miR-122-3p and EZH2 Expressions in Femoral Head Tissue by Real-Time Fluorescent Quantitative Polymerase Chain Reaction**

Femoral head tissue (50 mg) was collected from each group and lysed with 1 mL of lysis buffer. Thereafter, the tissue was cut into pieces with small scissors, and fully homogenised with a homogeniser. Total RNA was extracted from the tissue following the extraction procedures, and the concentration of total RNA was measured to analyse its integrity. A total of 16  $\mu$ L of total RNA was collected from each group, prepared into a 40  $\mu$ L system combined with other agents in the reverse transcription kit, and then reversely transcribed into cDNA. Later, the complete reverse cDNA was made into a template according to the instructions of the reagent, and amplified to a final volume of 20  $\mu$ L by PCR. The primer sequences for miR-122-3p were F: 5'-AA-CAGCACAACUACUACCUCA-3', R: 5'-UA-UUUAGUGUGAUAAUGGCGUU-3'; those for EZH2 were: F: 5'-CACCTACTACGACAAC-TCT-3', R: 5'-TGCGATGACACTGGATTC-3'; those for U6 were: F: 5'-CTCGCTTCGGCAGCA-CA-3', R: 5'-AACGCTTCACGAATTTGCGT-3'. The reaction was carried out at a temperature of 37°C for a duration of 30 minutes, followed by a temperature of 95°C for 20 seconds, another 95°C for 10 seconds, and finally a temperature of 60°C for 20 seconds. This process was repeated for a total of 40 cycles. Statistical analysis was performed using the Ct values obtained from relative quantification.

#### **Hematoxylin and Eosin (HE) Staining**

The mouse's two thigh bones were numbed using 5 percent chloral hydrate, then preserved with 4 percent formaldehyde for 72 hours at room

temperature, and finally decalcified at room temperature using 10 percent EDTA. Following the dehydration process using an ethanol gradient, the tissue was immersed in paraffin, sliced thinly (with a thickness of 4  $\mu$ m), and then placed in an incubator for a duration of 20 minutes. Following the removal of paraffin, the tissue was subjected to a 10-minute hematoxylin staining, then washed with flowing water until the tissue acquired a blue hue. Subsequently, the tissue underwent ethanol gradient dehydration once more, followed by a 2-minute eosin staining. Thereafter, it was dried, labelled and sealed with pine tar.

#### **Micro-CT**

Samples of the femur from every group were placed inside the test tube of the micro-CT system. The system's image resolution was configured as 2048  $\times$  1024, with a pixel size of 20 Lm  $\times$  20 Lm, and a layer spacing of 20 Lm. COBRA, a built-in software of the system, was utilized to measure the pertinent parameters: trabecular spacing (Tb.Sp), bone volume (BV), total volume (TV), bone volume fraction (BV/TV), trabecular thickness (Tb.Th), structure model index (SMI), trabecular number (Tb.N), and bone surface/bone volume (BS/BV).

#### **Fluorescence Detection of Target Gene through Dual Luciferase Reporter Assay**

TargetScan7.1, an online software for predicting target genes, revealed that miR-122-3p potentially targets EZH2. The 3'-UTR region of EZH2 contains binding sites for miR-122-3p. The original sequence of the wild type (EZH2 3'-UTR-WT) and the mutated type (EZH2 3'-UTR-MUT) were created and synthesized. These gene fragments were then inserted into the pmir-GLO luciferase reporter gene vector in order to build the EZH2 3'-UTR dual luciferase reporter gene vector (pmir-GLO-wt-survivin) and its corresponding mutant vector (pmir-GLO-mut-survivin).

After co-transfection of the recombinant vector plasmids and miR-122-3p mimics (miR-132) or miR-122-3p empty plasmids (NC) into BMSCs using Lipofectamine<sup>TM</sup> 3000, the luciferase activity was measured 48 hours later. Table 1 displays the grouping of co-transfection.

**Table 1: Co-transfection grouping**

Co-transfection	
NC	pmir GLO-wt-EZH23'-UTR
miR-122-3p	pmir GLO-wt-EZH23'-UTR
NC	pmir GLO-mut-EZH23'-UTR
miR-22-3p	pmir GLO-mut-EZH23'-UTR

Source: Authors

### Detection of EZH2 Expression in Femoral Tissue by Western Blotting

In each group, 200 mg of femoral head tissue was collected, shredded on ice, lysed with lysis solution, and centrifuged for 10 minutes at 4°C and 12,000 rpm. Next, the serum from the upper layer was collected, and the total protein concentration was measured using the BCA technique. Afterwards, the protein specimen underwent 12 percent SDS-PAGE and was subsequently transferred onto a PVDF membrane. The membrane was obstructed using 5 percent skim milk powder and subjected to primary antibodies (1:800) for 1 hour at 4°C, then incubated with secondary antibodies (1:2,000) for 1 hour at room temperature. In the end, the enhanced ECL system kit was utilized to observe all bands, with  $\beta$ -actin serving as the internal reference, and the band density was analysed using the ImageJ software.

### Effect of pCDNA3.1-EZH2 on Influence of miR-122-3p Overexpression on micro-CT 3D Reconstruction Parameters

The femoral medullary cavity was transfected with pCDNA3.1 (miR-122-3p group) and pCD-

NA3.1-EZH2 (miR-122-3p+EZH2 group) along with the introduction of MiR-122-3p mimics. To measure the relevant parameters, the femur samples from both groups were placed in the micro-CT system's test tube.

### Statistical Analysis

Statistical analysis was performed using Graphpad Prism 8.0 software. The measurement data were represented as the average plus or minus the standard deviation. Intergroup comparison was conducted using one-way ANOVA, while comparison between groups was performed using the t-test. A statistically significant difference was observed when  $P < 0.05$ .

## RESULTS

### Isolation, Purification, Culture and Identification of BMSCs

After culture for 3 days, there were a small number of cells adhering to the wall, and the morphology changed, presenting an extended and spindle shape. On the 7<sup>th</sup> day of culture, there are more cell colonies. After passage, the spindle shape of BMSCs became larger, there were more binuclear or multinucleated cells, the cells reached 100 percent confluence, and even stratified cells appeared in some areas (Fig. 1A). In the third-generation BMSCs, a large number of positive cells for surface antigens CD29 and CD90 were observed by immunofluorescence staining, but there were no positive cells for CD34 (Fig. 1B-D).

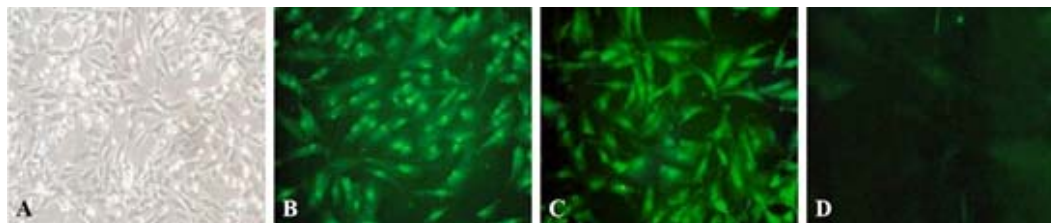


**Fig. 1. Immunofluorescence of third-generation BMSCs**

**A: Primary BMSCs cultured for 7 days ( $\times 400$ )**

**B: Third-generation BMSCs positive for surface antigen CD29 ( $\times 100$ )**

**C: Third-generation BMSCs positive for surface antigen CD90 ( $\times 100$ )**

**D: Third-generation BMSCs positive for surface antigen CD34 ( $\times 100$ )**

Source: Authors

### Expressions of miR-122-3p and EZH2 in Femoral Head Tissues

The miR-122-3p expression was significantly reduced and the EZH2 expression was increased in the ONFH and miR-NC groups compared to the Normal group ( $P < 0.05$ ). In the miR-122-3p group, the level of miR-122-3p was elevated, whereas the level of EZH2 was decreased compared to the ONFH group ( $P < 0.05$ ). There were no notable disparities observed in the levels of miR-122-3p and EZH2 between the ONFH and miR-NC groups ( $P > 0.05$ ) (Fig. 2).

### Histomorphology of Femoral Head Tissue and micro-CT 3D Reconstruction Parameters

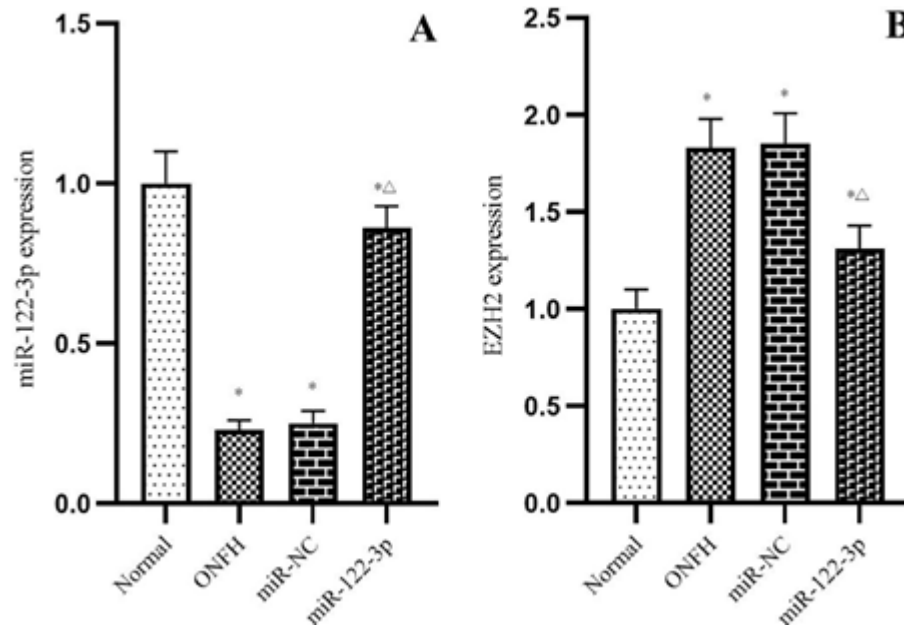
In comparison with the Normal group, ONFH and miR-NC groups had smaller trabecular coefficient, disordered structure, broken trabecular bones, more trabecular fracture, local dispersed distribution of empty lacunae in the femoral head, and larger trabecular space. The miR-122-3p

group had significantly improved local trabecular structure of the femoral head, normal trabecular structure, reduced trabecular fracture, and parallel arrangement, consistent direction, and decreased spacing of trabecular bones (Fig. 3).

Tb.Sp, SMI, and BS/BV were significantly higher in the ONFH and miR-NC groups compared to the Normal group, while BV/TV, Tb.Th, and Tb.N were significantly lower ( $P < 0.05$ ). Compared to the ONFH group, the miR-122-3p group exhibited significantly reduced Tb.Sp, SMI, and BS/BV, while showing increased BV/TV, Tb.Th, and Tb.N ( $P < 0.05$ ). Nevertheless, there were no notable disparities in the trabecular structure parameters between the ONFH and miR-NC groups ( $P > 0.05$ ), as indicated in Table 2.

### Prediction and Identification of Targeting Relationship of miR-122-3p

Figure 4A shows the presence of base complementary binding sites between miR-122-3p and the 3'-UTR of EZH2. The luciferase assay re-

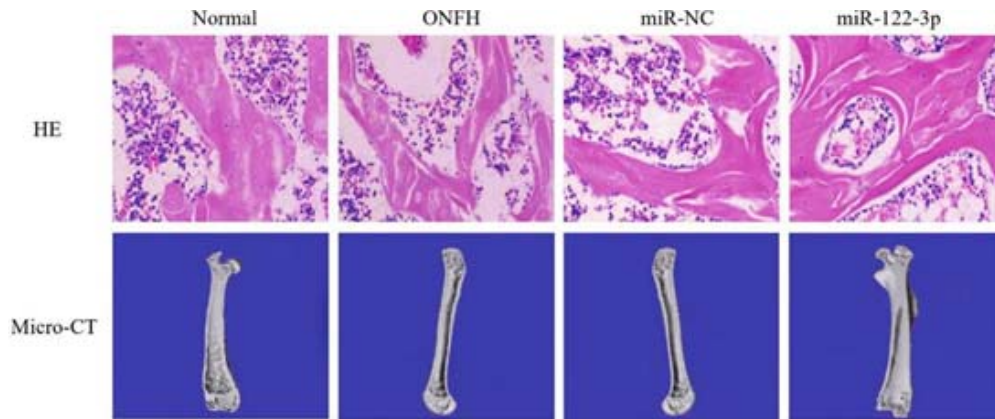
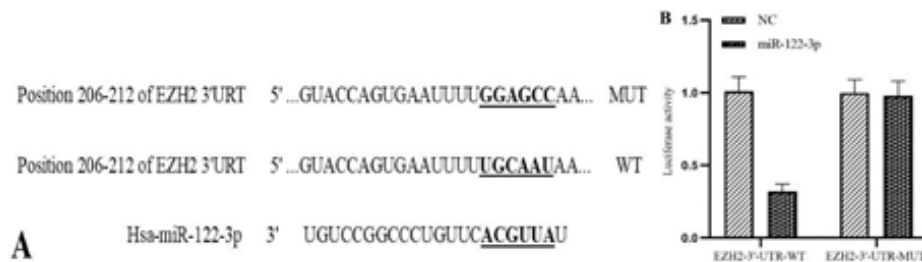


**Fig. 2.** Expressions of miR-122-3p and EZH2 in femoral head tissue of mice  
**A:** Comparison of the expressions of miR-122-3p in the femoral heads of mice across different groups  
**B:** Comparison of the expressions of EZH2 in the femoral heads of mice across different groups  
 \* $P < 0.05$  vs. NC group, \* $P < 0.05$  vs. ONFH group  
 Source: Authors

**Table 2: Trabecular Structure Parameters ( $\bar{x} \pm s$ , n=10)**

Group	Tb.Sp (mm)	BV/TV	Tb.Th (mm)	SMI	Tb.N	BS/BV (1/mm)
Normal	0.31±0.02	0.41±0.03	0.21±0.03	0.57±0.06	3.25±0.11	16.73±1.46
ONFH	0.42±0.05*	0.15±0.02*	0.13±0.02*	1.32±0.11*	2.04±0.08*	20.45±2.01*
miR-NC	0.43±0.06*	0.16±0.02*	0.15±0.02*	1.35±0.12*	2.01±0.07*	21.67±2.04*
miR-122-3p	0.36±0.03**	0.37±0.03**	0.19±0.03**	0.62±0.08**	2.96±0.10**	17.93±1.72**
F	16.94	287.6	20.51	200.7	482.6	15.43
P	<0.0001	<0.0001	<0.0001	<0.0001	<0.0001	<0.0001

\*P<0.05 vs. NC group, \*\*P<0.05 vs. ONFH group

**Fig. 3. HE staining ( $\times 400$ ) of femoral head tissue and micro-CT 3D reconstruction****Fig. 4. Targeting relationship between miR-122-3p and EZH2**

**A:** Online prediction of the binding sites between EZH2 and miR-122-3p

**B:** Luciferase assay to confirm the targeting relationship between EZH2 and miR-122-3p

Source: Authors

sults showed that transfection of wild-type EZH2 (EZH2-WT) resulted in a significant decrease in luciferase activity in the miR-122-3p group compared to the NC group ( $P < 0.05$ ). Nevertheless, there was no notable disparity observed in the luciferase function between miR-122-3p and NC groups subsequent to the co-transfection of mutant EZH2 (EZH2-MUT) ( $P > 0.05$ ) (Fig.4B).

### Expression of EZH2 in Femoral Head Tissue

EZH2 protein expression was significantly higher in the ONFH and miR-NC groups than in the Normal group ( $P < 0.05$ ). The miR-122-3p group exhibited a notable decrease in EZH2 protein expression compared to the ONFH group ( $P < 0.05$ ) (Fig. 5).

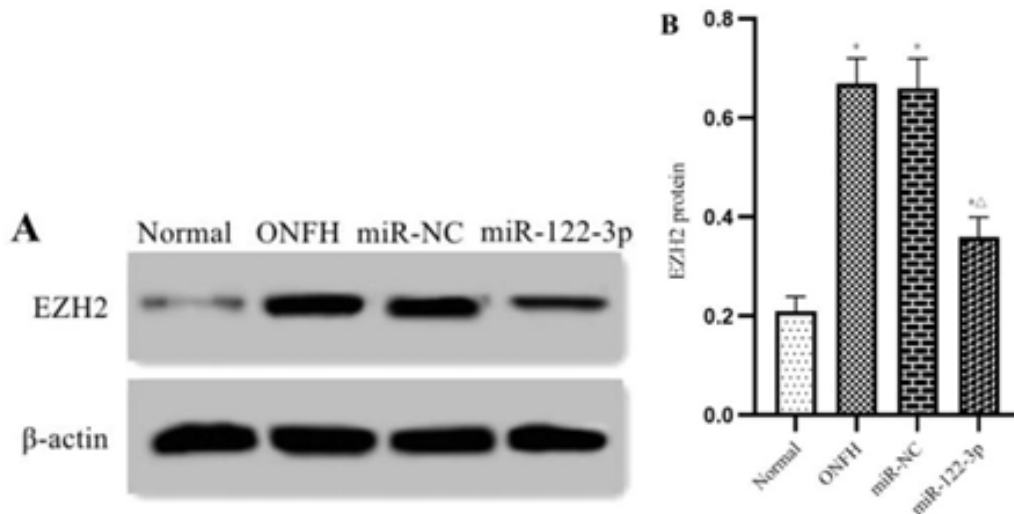


**Fig. 5. Protein expression of EZH2 in femoral head tissue of mice**  
**A: Protein expression of EZH2 in femoral head tissue of mice**  
**B: Comparison of protein expression of EZH2 in femoral head tissue of mice among groups**  
 Source: Authors

#### Effect of pCDNA3.1-EZH2 Transfection on Influence of miR-122-3p Overexpression on micro-CT 3D Reconstruction Parameters

The miR-122-3p + EZH2 group exhibited higher Tb.Sp, SMI, and BS/BV, while showing lower BV/TV, Tb.Th, and Tb.N compared to the miR-122-3p group ( $P < 0.05$ ). Thus, pCDNA3.1-EZH2 has the ability to counteract the impact of miR-122-3p overexpression on the parameters of trabecular structure (Fig. 6).

#### DISCUSSION

Most ONFH patients suffer from femoral head collapse within 4 years after missing timely and effective treatment in the early stage, so hip joint injury easily occurs (Li et al. 2019). Hence, finding effective therapy for ONFH has been highlighted. The response of humans to glucocorticoids is basically similar to that of animals, and the ideal model of SIONFH lays a foundation for studying the pathogenesis (Kong et al. 2020). In this study, a mouse model of SIONFH was constructed by using lipopolysaccharide. The results of HE staining showed increased

empty bone lacunae, severe trabecular destruction, and obviously reduced trabeculae, indicating successful modelling.

By binding target mRNA 3'-UTR, miRNA can suppress mRNA translation and promote its degradation (Rahman et al. 2021). MiRNA can modulate cell proliferation, differentiation and apoptosis (Wu et al. 2020; Yang et al. 2020). Bioinformatics analysis verifies that miRNAs may regulate most human genes, suggesting an important role in gene expression (Xiong et al. 2020). MiRNAs have directly been involved in the pathogenesis of osteosarcoma, osteonecrosis, and osteoarthritis (Xu et al. 2020). MiRNA expression usually has disorders in the necrotic tissues and BMSCs of patients or animal models with SIONFH (Kong et al. 2019). Zhao et al. (2019) found that the expressions of miR-452-3p, miR-601, and miR-647 were significantly up-regulated while miR-122-3p expression was lowered in the model group compared with those in control group during osteogenic differentiation. Likewise, miR-122-3p expression decreased in the case of SIONFH. Moreover, ONFH can be diagnosed based on elevated empty lacuna rate and osteopenia of the femoral head (Li and Wang

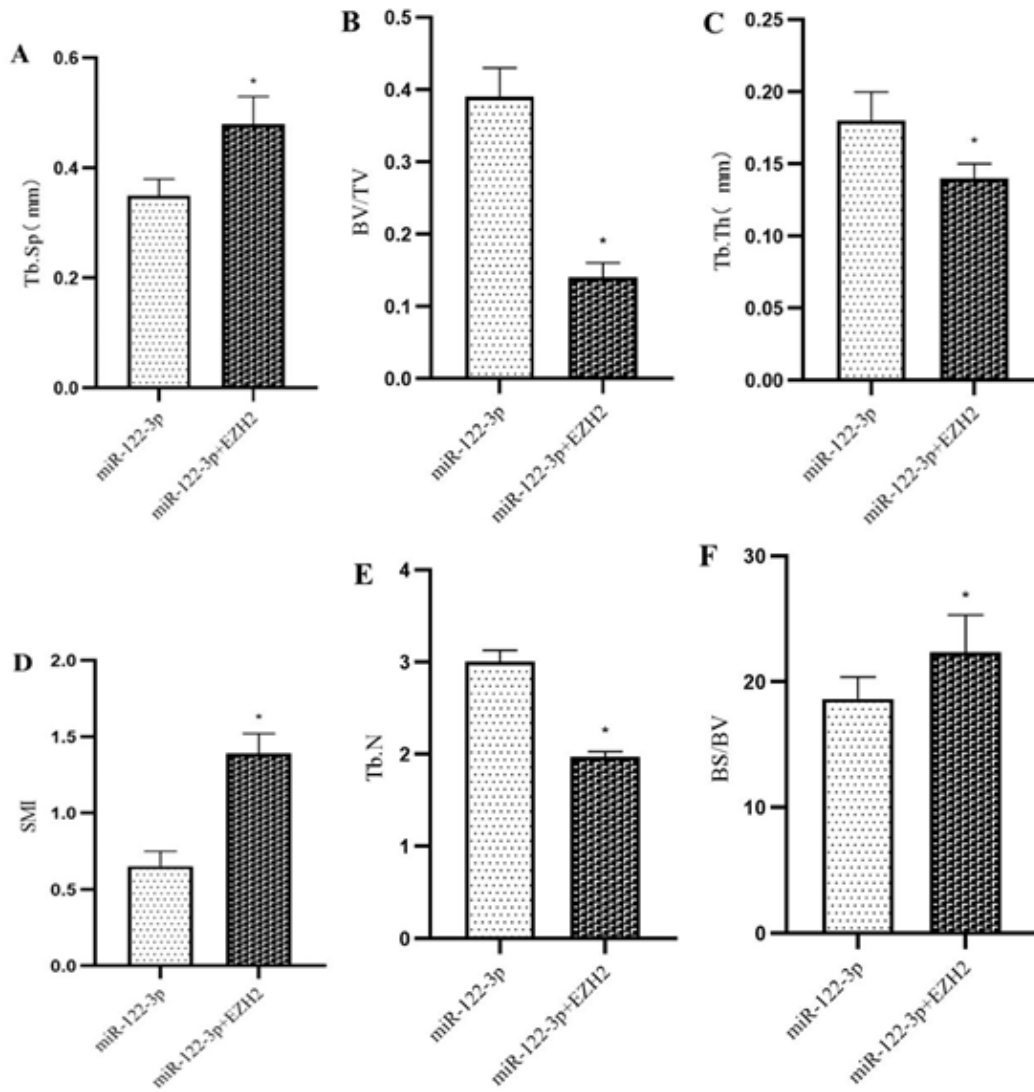


**Fig. 6. Trabecular parameters**

**A:** Comparison of Tb.Sp

**B:** Comparison of BV/TV

**C:** Comparison of Tb.Th

**D:** Comparison of SMI

**E:** Comparison of Tb.N

**F:** Comparison of BS/BV

\*P<0.05 vs. miR-122-3p group

2019). In this study, miR-122-3p overexpression improved trabecular parameters, thus relieving ONFH.

MiRNAs play various biological roles by affecting the expressions of downstream genes, and one miRNA may target many genes in dif-



ferent tissues and physiological processes (Akbari et al. 2020). Herein, miR-122-3p targeted the EZH2 gene in SIONFH. The EZH2 gene has many different functional domains and can modify chromosomes (Stasik et al. 2020). It not only mediates the onset and progression of bone and joint diseases, but also is highly expressed in articular cartilage (Xu et al. 2022). Suppressing EZH2 expression is capable of decreasing the matrix-degrading enzyme synthesis through the chondrocytes in mice, thus inhibiting the progression of arthritis (Allas et al. 2020). Herein, the protein expression of EZH2 was un-regulated in SIONFH, and EZH2 reversed the influence of miR-122-3p on the trabecular parameters of ONFH tissue, implying a negative regulatory role of miR-122-3p in EZH2 expression.

### CONCLUSION

In summary, miR-122-3p plays an inhibitory role in ONFH, and its expression is lowered in SIONFH. The overexpression of miR-122-3p can relieve SIONFH through negatively regulating EZH2.

### RECOMMENDATIONS

Further in vitro and clinical studies are still in need to validate the findings of this study.

### ACKNOWLEDGMENTS

This study was financially supported by the Science and Technology Project of Shenzhen (No. JCYJ20190813113201660) and Project of Health Bureau of Pingshan District, Shenzhen (No. 201909).

### ABBREVIATIONS

BMSC: bone marrow mesenchymal stem cell  
BS/BV: bone surface/bone volume  
BV: bone volume  
BV/TV: bone volume fraction  
CD: cluster of differentiation  
DMEM: Dulbecco's modified Eagle medium  
EZH2; enhancer of zeste homologue 2  
HE: hematoxylin and eosin  
LPS: lipopolysaccharide  
miRNA: micro ribonucleic acid

mRNA: messenger RNA  
ONFH: osteonecrosis of the femoral head  
SIONFH: steroid-induced ONFH  
SMI: structure model index  
Tb.N: trabecular number  
Tb.Sp: trabecular spacing  
Tb.Th: trabecular thickness  
TV: total volume  
3'-UTR: 3'-untranslated region

### REFERENCES

- Akbari A, Majd HM, Rahnama R et al. 2020. Cross-talk between oxidative stress signaling and microRNA regulatory systems in carcinogenesis: Focused on gastrointestinal cancers. *Biome Pharmacother*, 131: 110729.
- Allas L, Brochard S, Rochoux Q et al. 2020. EZH2 inhibition reduces cartilage loss and functional impairment related to osteoarthritis. *Sci Rep*, 10(1): 19577.
- Aranza-Martínez A, Sánchez-Pérez J, Brito-Elias L et al. 2021. Non-coding RNAs associated with radioresistance in triple-negative breast cancer. *Front Oncol*, 11: 752270.
- Baba S, Motomura G, Ikemura S et al. 2020. Quantitative evaluation of bone-resorptive lesion volume in osteonecrosis of the femoral head using micro-computed tomography. *Joint Bone Spine*, 87(1): 75-80.
- Chen CY, Du W, Rao SS et al. 2020. Extracellular vesicles from human urine-derived stem cells inhibit glucocorticoid-induced osteonecrosis of the femoral head by transporting and releasing pro-angiogenic DMBT1 and anti-apoptotic TIMP1. *Acta Biomater*, 111: 208-220.
- Chikvatia L, Avazashvili N, Obgaidze G et al. 2020. Steroid-induced osteonecroses of femoral head. *Georgian Med News*, 298: 21-27.
- Chu W, Zhang X, Qi L et al. 2020. The EZH2-PHACTR2-AS1-ribosome axis induces genomic instability and promotes growth and metastasis in breast cancer. *Cancer Res*, 80(13): 3326.
- Deng P, Yu Y, Hong C et al. 2020. Growth differentiation factor 6, a repressive target of EZH2, promotes the commitment of human embryonic stem cells to mesenchymal stem cells. *Bone Res*, 8(1): 39.
- Hao W, Liu HZ, Zhou LG et al. 2019. MiR-122-3p regulates the osteogenic differentiation of mouse adipose-derived stem cells via Wnt/ $\beta$  catenin signaling pathway. *Eur Rev Med Pharmacol Sci*, 23(9): 3892-3898.
- Hua KC, Yang XG, Feng JT et al. 2019. The efficacy and safety of core decompression for the treatment of femoral head necrosis: A systematic review and meta-analysis. *J Orthop Surg Res*, 14: 306.
- Kang JS, Suh YJ, Moon KH et al. 2018. Clinical efficiency of bone marrow mesenchymal stem cell implantation for osteonecrosis of the femoral head: A matched pair control study with simple core decompression. *Stem Cell Res Ther*, 9: 274.
- Kong L, Zuo R, Wang M et al. 2020. Silencing microRNA-137-3p, which targets RUNX2 and CXCL12 pre-

- vents steroid-induced osteonecrosis of the femoral head by facilitating osteogenesis and angiogenesis. *Int J Biol Sci*, 16(4): 655-670.
- Kong LC, Guan JJ, Kang QL. 2019. Research progress on the role of miRNA in hormone-induced femoral head necrosis. *J Orthopaedics*, 40(4): 5.
- Lai SW, Lin CL, Liao KF. 2020. Evaluating the association between avascular necrosis of femoral head and oral corticosteroids use in Taiwan. *Medicine*, 99(3): e18585.
- Li MD, Yang F, Chen HJ et al. 2019. Asparaginase intervention can promote ischemia and necrosis of femoral head in hormone-induced model mice. *Chinese Tissue Engineering Res*, 23(27): 6.
- Li WJ, Wang QG. 2019. Clinical study on the treatment of femoral head necrosis with partially collapsed femoral head by femoral head and neck fenestration. *World Compound Med*, 5(4): 154-156.
- Liao W, Ning Y, Xu HJ et al. 2019. BMSC-derived exosomes carrying microRNA-122-5p promote proliferation of osteoblasts in osteonecrosis of the femoral head. *Clin Sci (Lond)*, 133(18): 1955-1975.
- Naik AA, Narayanan A, Khanchandani P et al. 2020. Systems analysis of avascular necrosis of femoral head using integrative data analysis and literature mining delineates pathways associated with disease. *Sci Rep*, 10(1): 18099.
- Pavelka T, Saláček M, Bárta P et al. 2019. Avascular necrosis of femoral head and coxarthrosis progression after acetabular fractures. *Acta Chir Orthop Traumatol Cech*, 86(6): 381-389.
- Rahman F, Akand SK, Faiza M et al. 2021. miRNA target prediction: Overview and applications. In: S Hameed, Z Fatima (Eds.): *Integrated Omics Approaches to Infectious Diseases*. Singapore: Springer, pp. 241-253.
- Stasik S, Middeke JM, Kramer M et al. 2020. EZH2 mutations and impact on clinical outcome: An analysis in 1,604 patients with newly diagnosed acute myeloid leukemia. *Haematologica*, 105(5): e228-e231.
- Wang A, Ren M, Song Y et al. 2018. MicroRNA expression profiling of bone marrow mesenchymal stem cells in steroid-induced osteonecrosis of the femoral head associated with osteogenesis. *Med Sci Monit*, 24: 1813-1825.
- Wang SL, Hu YB, Chen H et al. 2020. Efficacy of bone marrow stem cells combined with core decompression in the treatment of osteonecrosis of the femoral head: A PRISMA-compliant meta-analysis. *Medicine*, 99(25): e20509.
- Wu F, Wang F, Yang Q et al. 2020. Upregulation of miRNA-23a-3p rescues high glucose-induced cell apoptosis and proliferation inhibition in cardiomyocytes. *In Vitro Cell Dev Biol Anim*, 56(10): 866-877.
- Xiong Y, Chen L, Yan C et al. 2020. M2 macrophagy-derived exosomal miRNA-5106 induces bone mesenchymal stem cells towards osteoblastic fate by targeting salt-inducible kinase 2 and 3. *J Nanobiotechnology*, 18(1): 66.
- Xu F, Li W, Yang X et al. 2021. The roles of epigenetics regulation in bone metabolism and osteoporosis. *Front Cell Dev Biol*, 8: 619301.
- Xu T, Luo Y, Wang J et al. 2020. Exosomal miRNA-128-3p from mesenchymal stem cells of aged rats regulates osteogenesis and bone fracture healing by targeting Smad5. *J Nanobiotechnology*, 18(1): 47.
- Xu WD, Huang Q, Huang AF. 2022. Emerging role of EZH2 in rheumatic diseases: A comprehensive review. *Int J Rheum Dis*. doi: 10.1111/1756-185X.14416.
- Yang Y, Yujiao W, Fang W et al. 2020. The roles of miRNA, lncRNA and circRNA in the development of osteoporosis. *Biol Res*, 53(1): 40.
- Zhao SR, Wen JJ, Mu HB. 2019. Role of Hsa-miR-122-3p in steroid-induced necrosis of femoral head. *Eur Rev Med Pharmacol Sci*, 23(3 Suppl): 54-59.

Paper received for publication in December, 2021  
 Paper accepted for publication in April, 2022